Bol. Soc. Paran. Mat.
©SPM – E-ISSN-2175-1188
SPM: www.spm.uem.br/bspm

(3s.) **v. 2026 (44) 2** : 1–14.
ISSN-0037-8712
doi:10.5269/bspm.80496

Investigation of MHD flow with Viscous Dissipation, Heat Source, and Soret Effects on a Vertical Moving Plate

[1] Rajeswari Sowmya Cheruvu,[2] Bala Siddulu Malga,[3] Gadipalli Deepa,[4] Gitti Narsimlu

ABSTRACT: The current research investigates the impact of viscous dissipation, thermal convection, and the Soret effect on an incompressible aqueous ionic fluid on MHD boundary layer flow over a moving plate vertically. By applying the similarity transformations, the governing partial differential equations are converted into a system of ordinary differential equations, using the fourth-order Runge-Kutta integration method in conjunction with the shooting technique. A detailed graphical analysis is depicted to illustrate the various physical characteristics of temperature, concentration, and velocity profiles on dimensionless parameters as Prandtl, Magnetic parameter, Eckert number, Chemical reaction, Grashof number, and modified Grashof number. Also, variations in Nusselt number, Skin-friction coefficient, and Sherwood coefficients were observed to assess the impact on heat and mass parameters.

Keywords: Soret effect, viscous dissipation, vertical moving plate, heat source, chemical reaction.

Contents

1. Introduction

In recent years, the research on MHD Boundary layer flow analysis of mass and heat transport has gained significant interest for its theoretical and practical applications in industries of Power generators for converting kinetic and thermal energy into electrical energy using magnetic fields, polymer extrusion for extruders to process molten polymers through dies, chemical reactors for handling ionized gases or liquids, cooling systems for circulating the conducting fluids under magnetics influence for heat removal, Electro-chemical reactors for electrolysis, plating, and electrochemical synthesis using ionic fluids Fe2+, in nuclear reactors for conducting coolant interactions with magnetics fields in electromagnetic pumps, also for Biomedical Devices for magnetically actuated microchannels used for blood flow. A study of Viscous dissipation with chemical reaction over a radially extending axisymmetric flow using similarity transformations is detailed by S. Renuka [1]. Investigation of viscous fluid flow over an exponentially extending porous sheet with Joule heating, velocity slip on magnetic field effects is given by Srinivasacharya [2]. Description of MHD mixed convection with mass and heat transfer on an infinite vertical plate over a porous medium with chemical reaction, heat source, and Joule heating is explained by Ibrahim [3]. Analysis of axisymmetric MHD flow over a radially stretching sheet with Heat and Mass transfers using governing equations is explained by Hayat [4]. A viscous incompressible and Ionic aqueous solution along an infinite vertical plate on porous medium with Mass and Heat absorption with radiation effect is detailed by Mangamma [5], an unsteady free convection heat transfer on a vertical porous plate with the chemical reaction, thermal radiation, and temperature variation is detailed by Mangamma [6]. Joule heating and non-uniform source/sink effects in MHD mixed convection flow over a vertical stretching

2020 *Mathematics Subject Classification:* 76D10, 76W05.
Submitted November 30, 2025. Published March 14, 2026

surface in a Darcy–Forchheimer porous medium were explained by B.K. Sharma [7]. The viscous dissipation on an axisymmetric rotating channel has been explained by Awais [8]. Chemical reaction on radially axisymmetric flow has been explained by Nayak [9]. Chemical reaction and Heat sink, adding viscous dissipation effect, have been studied by Matta [10].

Joule heating for mixed convective hydromagnetic flow is observed by Ahmed [11]. Electroosmotic mixed convection flow in microchannels under asymmetric heating with viscous dissipation and Joule heating was reported by Michael [12]. Radiation effects, heat and mass transfer with Soret and Dufour effects were observed by Kumar P.P. [13]. Soret application on concentration has been studied by Pramod [14]. Adding to this, Joule heating and viscous dissipation on a revolving disk have been observed by Sadia [15]. Joule heating and viscous dissipation effects in stretching sheet flows with the Soret effect were discussed by B.K. Swain [16]. The influence of dissipative Newtonian fluid on a thinner surface has been observed by Ravuri [17]. Exact solutions for induced flows over circular cylinders were presented by Turkyilmazoglu [18]. At the same time, the Ion slip effect and chemical reaction on a uniform wall temperature have been observed by Krishna [19]. Magneto-Hydrodynamic flow with viscous dissipation and internal heat generation is studied by Hussain [20]. MHD flows with Dufour and viscous dissipation effects on porous plates with chemical reactions were further studied by Behshad [21] and Mangamma [22]. Soret and Dufour effects for a steady flow have been examined by Mangamma [23]. and periodic analysis of thermal and magnetic effects on conducting fluids with Joule heating was again addressed by Nidhal [24]. The previous work supported the observations of the different parameters, such as the Heat Source, the Grashof method, the modified Grashof method, Prandtl, Eckert, Soret, and chemical reaction. In the context of MHD boundary layer flow of an incompressible aqueous ionic solution, including Soret, Heat source, viscous dissipation and Chemical reaction effects. It fills the gap of incorporating the effects of the Soret parameter with Grashof, modified Grashof, Heat source, viscous dissipation and chemical reaction on a vertical plate of moving surface. Soret parameter influences the temperature gradient affecting the mass diffusion, resulting the concentration variations in the presence of chemical reaction as Ferrous ion. Also, the introduction of a heat source makes the study of thermal conductivity simple. The similarity transformation method helps to derive accurate solutions. The graphs are estimated using the Runge-Kutta fourth-order and shooting technique. The results include the analysis of the Heat Source effect, Soret, and chemical reaction on Velocity, temperature, and concentration profiles have been observed.

Researching numerous studies on MHD boundary layer flows on heat and mass transfer, there are limited on the mixed effects of Soret effect, viscous dissipation, including heat generation and on vertical moving plates with chemical reactions. The current research fills the gap by providing coupled physical mechanisms.

2. Problem Formulation

Considering the conditions like diffusion–thermodynamic effects, viscous dissipation, and a heat source in an MHD flow. Thermal and concentration buoyancy effects are incorporated through the Grashof number and the modified Grashof number, respectively. A non-uniform transverse magnetic field of strength B0 is applied along the y-axis. Since the Reynolds number of the flow is assumed to be very low, the induced magnetic field can be neglected in comparison to the applied magnetic field. Furthermore, it is assumed that no external electric field exists outside the flow domain, which implies that charge polarisation is negligible. T_∞ and C_∞ denote the ambient fluid values of temperature and concentration. In contrast, the plate surface temperature and concentration are represented as Tw(x) and Cw(x), respectively. By invoking the Boussinesq approximation, the fluid properties are considered constant except for the density variation in the buoyancy terms of the momentum equation. The governing equations are estimated assuming the flow is incompressible, laminar, and two-dimensio-nal. The transverse magnetic field acts normal to the plate, with negligible induced field effects. heating and viscous dissipation are included in the energy balance. Heat source/sink effects are considered. Chemical reactions influence the concentration field. The Soret effect is included in the energy and concentration equations, respectively.

Figure 1 illustrates the magnetohydrodynamic (MHD) boundary-layer flow over a vertically stretching sheet with simultaneous heat and mass transfer. The sheet is aligned along the x-axis, and its stretching velocity is prescribed as u = Bx, where B is a constant. The ambient fluid flows vertically upward toward the free stream, developing a boundary layer adjacent to the sheet. Within the boundary layer, the

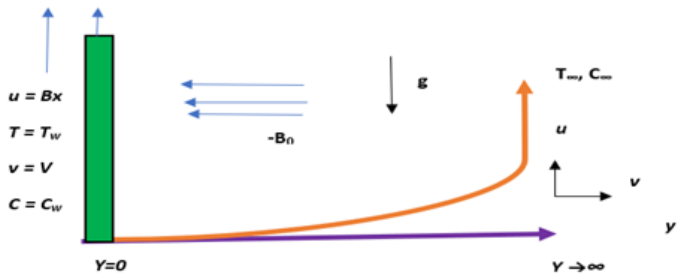

Figure 1: Physical Representation

fluid velocity components are denoted as u (tangential to the sheet) and v (normal to the sheet). The tangential velocity component u increases with distance away from the plate due to the stretching action. In contrast, the normal velocity component v adjusts to satisfy the continuity condition, varying across the boundary layer thickness. A transverse magnetic field B0, oriented normal to the flow direction, interacts with the electrically conducting fluid. The Lorentz force generated by this magnetic field opposes the fluid motion, thereby decelerating the velocity field and modifying the boundary layer thickness. Consequently, the interplay between viscous, buoyancy, magnetic, and diffusive effects governs the observed velocity, temperature, and concentration distributions in the boundary layer.

The Governing Equations of boundary layer flow are observed as follows:

Continuity Equation:

$$\frac{\partial u}{\partial x} + \frac{\partial v}{\partial y} = 0$$

Velocity Equation:

$$u\frac{\partial u}{\partial x} + v\frac{\partial u}{\partial y} = \nu\frac{\partial^2 u}{\partial y^2} + g\beta_T(T - T_\infty) + g\beta_c(C - C_\infty) - \frac{\sigma}{\rho}B_0^2 u$$

Temperature Equation:

$$u\frac{\partial T}{\partial x} + v\frac{\partial T}{\partial y} = \alpha\frac{\partial^2 T}{\partial y^2} + \frac{Q_0}{\rho c_p}(T - T_\infty) + \frac{\mu}{\rho c_p}\left(\frac{\partial u}{\partial y}\right)^2 - \frac{\sigma}{\rho}B_0^2 u^2$$

Diffusion Concentration Equation:

$$u\frac{\partial C}{\partial x} + v\frac{\partial C}{\partial y} = D_m\frac{\partial^2 C}{\partial y^2} - K_1(C - C_\infty) + Sr\frac{\partial^2 T}{\partial y^2}$$

and given boundary constraints:

$$u = U_0 x, \quad v = V_0, \quad T = T_w = T_\infty + Ax, \quad C = C_w = C_\infty + Bx$$

$$u \to 0, \quad v \to 0, \quad C \to C_\infty, \quad T \to T_\infty \quad \text{as } y \to \infty$$

Using the new similarity transformations Equations (2), (3) & (4) may be nondimensionalized as follows:

$$\phi(\eta) = x\sqrt{U_0\nu}\, f(\eta), \quad \theta(\eta) = \frac{T - T_\infty}{T_w - T_\infty}, \quad \varphi(\eta) = \frac{C - C_\infty}{C_w - C_\infty}, \quad \eta = \sqrt{\frac{U_0}{\nu}}\, y$$

By the stream function definition $\phi(x, y)$, we have

$$u = \frac{\partial \phi}{\partial y} = xU_0 f'(\eta), \qquad v = -\frac{\partial \phi}{\partial x} = -\sqrt{U_0\nu}\, f(\eta). \tag{2.1}$$

Therefore, the continuity equation (1) is identically satisfied.

$$f'''(\eta) + f''(\eta)f(\eta) - (f'(\eta))^2 - Mf'(\eta) + Gr\,\theta(\eta) + Gc\,\varphi(\eta) = 0. \tag{2.2}$$

$$\theta''(\eta) + Pr\,f(\eta)\theta'(\eta) + Ec\,(f''(\eta))^2 + Q\,\theta(\eta) = 0. \tag{2.3}$$

$$\varphi''(\eta) + Sc\,f(\eta)\varphi'(\eta) - K_c\varphi(\eta) + Sr\,\theta''(\eta) = 0. \tag{2.4}$$

For below governing equations below, the following physical boundary conditions are satisfied.

$$f(0) = -f_w, \quad f'(0) = 1, \quad \theta(0) = 1, \quad \varphi(0) = 1; \qquad f(\eta) \to 0, \quad \theta(\eta) \to 1, \quad \varphi(\eta) \to 1 \quad \text{as } \eta \to \infty. \tag{2.5}$$

By substituting the Grashof number for heat transport as

$$Gr = \frac{g\beta_T(T_w - T_\infty)}{xU_0^2},$$

the mass transfer Grashof number as

$$Gc = \frac{g\beta_C(C_w - C_\infty)}{xU_0^2},$$

the Prandtl number

$$Pr = \frac{\nu}{\alpha},$$

the Schmidt number

$$Sc = \frac{\nu}{D_m},$$

the chemical reaction parameter

$$K_c = \frac{k_1}{U_0},$$

the magnetic parameter

$$M = \frac{\sigma B_0^2}{\rho U_0},$$

the Eckert number

$$Ec = \frac{U_0^2}{(T_w - T_\infty)c_p},$$

the Soret number

$$Sr = \frac{D_m K_t(T_w - T_\infty)}{\nu T_m(C_w - C_\infty)},$$

and the local heat source parameter

$$Q = \frac{Q_0 b}{\gamma U_0}.$$

3. Methodology

The steps involved in solving the governing ordinary and partial differential equations are as follows:

- Formulation of the governing equations,
- Specification of the boundary conditions,
- Application of the similarity transformation method,
- Derivation of the non-dimensional equations,
- Numerical solution using the fourth-order Runge–Kutta method coupled with the shooting technique,

- Analysis of the results through graphical representation.

The Runge–Kutta fourth-order method is one of the most reliable and widely used numerical techniques for solving ordinary differential equations. The shooting method is employed to convert the boundary value problem into an equivalent initial value problem by guessing the unknown initial conditions that satisfy the boundary conditions at infinity.

Equations (2.2)–(2.4), together with the boundary conditions given in Equation (2.5), are solved numerically using this combined Runge–Kutta and shooting approach.

$$f = Y_1, \qquad f' = Y_2, \qquad f'' = Y_3, \qquad f''' = Y_2^2 + MY_2 - Y_1Y_3 - GrY_4 - GcY_6 \tag{3.1}$$

$$\theta = Y_4, \qquad \theta' = Y_5, \qquad \theta'' = -PrY_1Y_5 - PrEcY_3^2 - QY_4 \tag{3.2}$$

$$\phi = Y_6, \qquad \phi' = Y_7, \qquad \phi'' = -ScY_1Y_7 + K_cY_6 + Sr\left(PrY_1Y_5 + PrEcY_3^2 + QY_4\right) \tag{3.3}$$

Boundary conditions:

$$Y_1(0) = 0, \quad Y_2(0) = 1, \quad Y_2(\infty) = 0, \quad Y_4(0) = 1, \quad Y_4(\infty) = 0, \quad Y_6(0) = 1, \quad Y_6(\infty) = 0 \tag{3.4}$$

$$C_f = \frac{2\tau_w}{\rho U_0^2} \tag{3.5}$$

$$Nu = \frac{xq_w}{k(T_w - T_\infty)} \tag{3.6}$$

$$Sh = \frac{xq_m}{D(C_w - C_\infty)} \tag{3.7}$$

The wall mass flux, wall heat flux, and wall shear stress are defined respectively as:

$$\tau_w = \mu \left.\frac{\partial U}{\partial y}\right|_{y=0} \tag{3.8}$$

$$q_w = -k \left.\frac{\partial T}{\partial y}\right|_{y=0} \tag{3.9}$$

$$q_m = -D \left.\frac{\partial C}{\partial y}\right|_{y=0} \tag{3.10}$$

The drag, heat, and mass transfer relations are given by:

$$f''(0) = \rho x \left(\frac{\sqrt{C_0\nu}}{2u}\right) S_f \tag{3.11}$$

$$\theta'(0) = -\frac{1}{x}\sqrt{\frac{\nu}{C_0}}\, Nu \tag{3.12}$$

$$\phi'(0) = -\frac{1}{x}\sqrt{\frac{\nu}{C_0}}\, Sh \tag{3.13}$$

Mathematical calculations are performed using the computer-based software "MATLAB". Tables and Graphs were computed through MATLAB software. By using a very successful mathematical approach for the fourth-order Runge-Kutta system with the integration of shooting method is applied to solve transformed differential equations. The strategy of selection assumes the appropriate finite elements of $n \to \infty$. Using a set of parameters by selecting n_∞ requires suitable initial values to solve the problem for $f''(0)$, $\theta'(0)$, and $\phi'(0)$. To integrate the system of transformed differential equations, the fourth–order Runge–Kutta method is employed. The above procedure is repeated until the desired accuracy with an error tolerance of 10^{-5} is achieved.

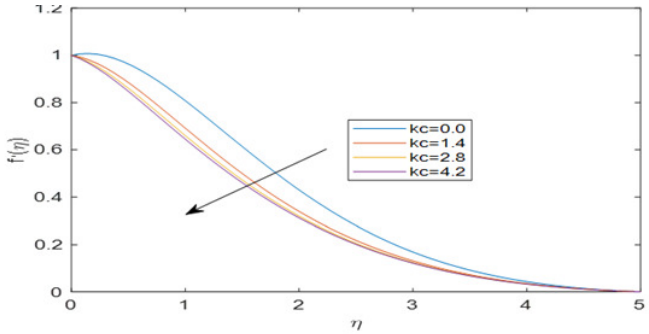

Figure 2: Velocity for different values of the Chemical Reaction

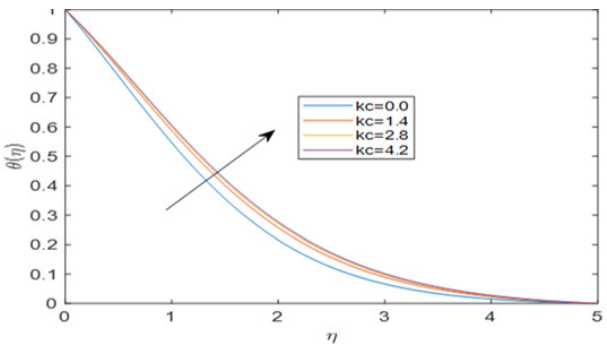

Figure 3: Temperature for different values of the Chemical Reaction

4. Results

The Shooting method with integration of the Runge Kutta method has been taken to solve the collection of Equations (2.2) - (2.5) numerically, considering the boundary conditions (3.4). To specify the problem, the following parameter values are taken into consideration: Gr =1, Gc=1, n=1, Sc=0.62, kc=0.5, Ec=0.2, Pr=0.72, M=1, Q=0.2 Parameters. The impacts of heat source parameter (Q), Eckert number (Ec), Modified Grashof number, Prandtl number (Pr), Grashof number, and Soret number (Sr) on temperature, velocity, and concentration profiles are presented in graphs below. For the graphical analysis to be numerically accurate, Grid independence and convergence tests are performed. It is estimated that the physical characteristics result in the graphs in temperature, concentration, and velocity profiles, and Nusselt, Skin-friction, and Sherwood coefficients were observed along different parameters like temperature, velocity, chemical reaction, Skinfriction, Nusselt and Sherwood parameters. Assuming fluids like aqueous ionic solution with the chemical as Fe+2 ions, the Momentum diffusivity is greater than the thermal diffusivity for fluids. Similarly, momentum is transported more efficiently than heat.

Figure 1: An increase in the chemical reaction parameter accelerates the consumption of diffusing species, thereby reducing solute concentration in the boundary layer. This reduction weakens solutal buoyancy forces, which play a key role in driving flow. As a result, the velocity near the plate decreases, and the velocity boundary layer becomes thicker. Hence, stronger chemical reactions suppress fluid motion. Similar findings were reported by Malga et al. [1], who noted that increasing Kc reduces velocity profiles in chemically reacting MHD convection flows.

Figure 2: Exothermic reactions release additional heat into the fluid, which enhances the thermal energy within the boundary layer. This increases fluid temperature and thickens the thermal boundary layer. In contrast, endothermic reactions absorb heat, reducing the thermal energy and lowering the temperature distribution. Thus, exothermic reactions lead to a temperature rise, while endothermic reactions cause a decrease. Malga et al. [1] also observed that, confirming the strong influence of reaction type on thermal behaviour in MHD convection flows.

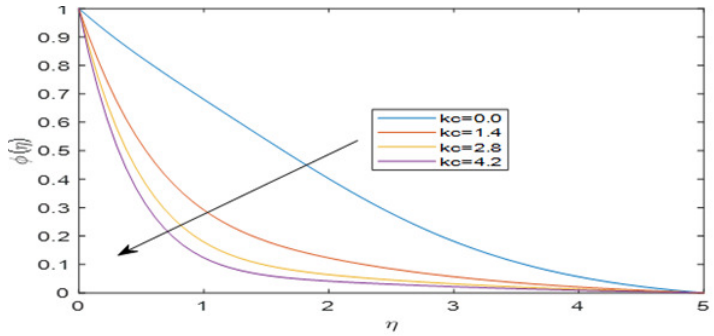

Figure 4: Concentration for different values of the Chemical Reaction

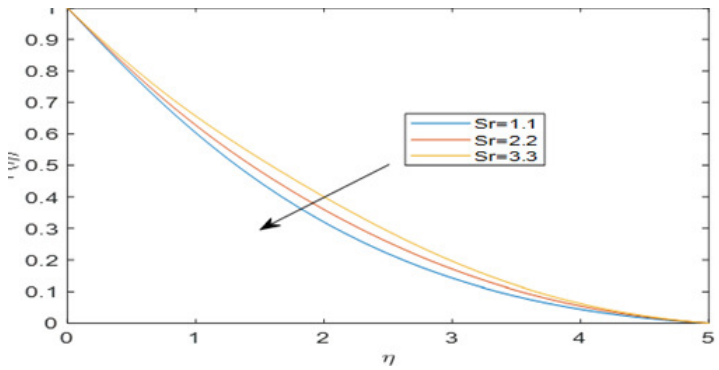

Figure 5: Velocity for different values of the Soret number

Figure 3: The presence of a chemical reaction alters the concentration field by consuming reactants and generating products within the boundary layer. This process intensifies mass diffusion and develops steeper concentration gradients. As a result, the overall concentration of the diffusing species decreases, leading to a thinner concentration boundary layer. Malga et al. [1] also observed that stronger reaction rates significantly reduce concentration profiles in reactive MHD convection flows.

Figure 4: The Soret effect (thermal-diffusion) enhances solute mass flux due to temperature gradients, thereby strengthening solutal buoyancy forces in the flow. As buoyancy increases, fluid velocities rise and the momentum boundary layer becomes thinner, with a greater potential for flow instabilities or turbulence at higher values. Consequently, velocity profiles increase with the Soret number. Mangamma [14] also observed that confirming that thermal-diffusion effects accelerate fluid motion in MHD mixed convection systems.

Figure 5: The Soret effect induces solute flux due to temperature gradients, which indirectly influences the thermal field. Enhanced thermal-diffusion causes steeper temperature gradients near the wall, improving heat transfer from the surface. As a result, the fluid temperature within the boundary layer decreases with increasing Soret number. Mangamma [14], who reported that stronger Soret effects enhance mass transfer while slightly reducing the temperature distribution in buoyancy-driven MHD flows.

Figure 6: The Soret effect induces solute migration due to temperature gradients, creating steeper concentration gradients within the boundary layer. This leads to thinner concentration layers and enhanced mass transfer. Consequently, as the Soret number increases, the concentration of the diffusing species near the wall rises. Mangamma [14], who demonstrated that higher Soret numbers strengthen solute distribution in buoyancy-driven MHD flows.

Figure 7: depicts the result of the skin friction coefficient with chemical reaction, as skin friction defines the shear stress at a fluid-solid interface, which results in dynamic pressure of the fluid, resulting in the reduction of species concentration near the plate, hence the buoyancy weakens, reducing the velocity gradients, which decreases the skin-friction. As a result, a rise in chemical reaction decreases Skin friction

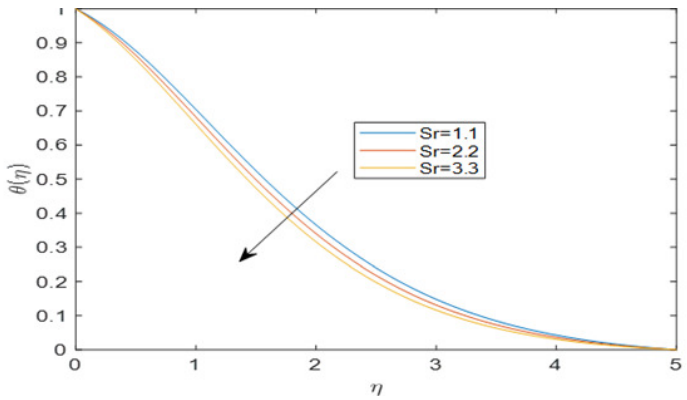

Figure 6: Temperature for different values of the Soret number

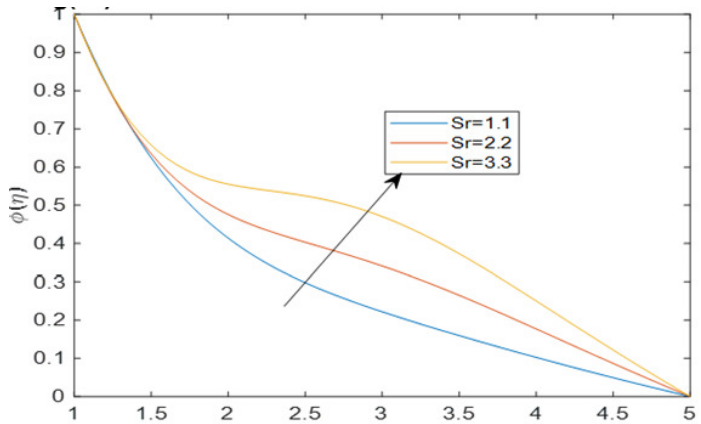

Figure 7: Concentration for different values of the Soret number

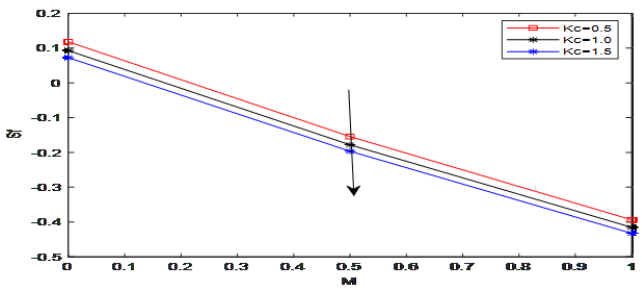

Figure 8: Skin friction coefficient on Chemical reaction

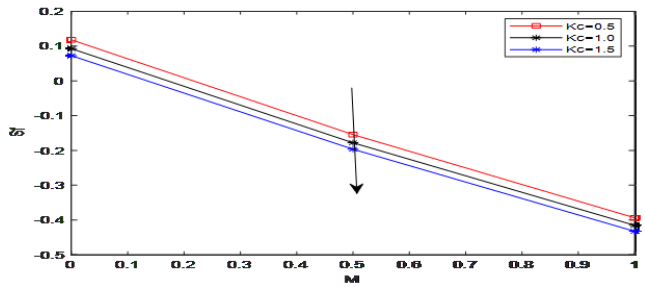

Figure 9: Skin Friction Coefficient on Schmidt Number

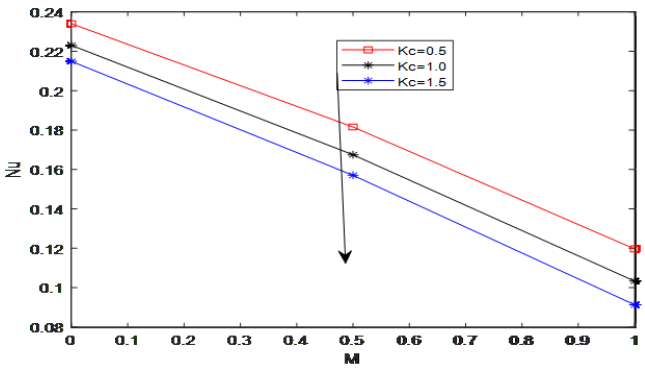

Figure 10: Nusselt number on Chemical Reaction

is also noted by Nayak [9].

Figure 8: depicts the result of the increase in Schmidt number, which makes a thinner concentration boundary layer. The velocity gradient near the surface decreases with reduced shear stress. The Skin friction coefficient reduces with the rise in Schmidt number, also observed by Malga et al. [1].

Figure 9: depicts the relation of Nusselt number on Chemical Reaction, chemical reaction reduces the concentration of species at wall, which reduces the heat transport as a result, Nusselt number decreases. Hence, as the Chemical reaction increases, the Nusselt number decreases, also observed by Malga et al. [1].

Figure 10: depicts that the higher Schmidt number reduces mass diffusivity, which reduces the species diffusion, resulting in a reduction of the concentration boundary layer. Reduction in temperature gradient occurs as the temperature boundary layer thickens. That reduces the heat transfer at the wall so that the Nusselt number decreases. Hence, the Nusselt number decreases with an increase in the Schmidt number, also observed by Malga et al. [1].

Figure 11: The Sherwood number represents the ratio of convective to diffusive mass transfer at the surface. An increase in the Schmidt number indicates that momentum diffusivity dominates over mass diffusivity, which reduces the rate of species diffusion. Consequently, the Sherwood number decreases as Sc rises, reflecting slower mass transfer. Similar trends have been reported by Karim [23], who showed that higher Schmidt numbers suppress mass transfer in MHD boundary-layer flows.

Figure 12: Stronger chemical reactions consume the diffusing species more rapidly, reducing concentration gradients within the boundary layer. This diminishes the mass transfer rate, leading to a lower Sherwood number. Conversely, decreasing the chemical reaction rate allows higher concentration gradients, thereby increasing the Sherwood number. Similar observations were reported by Karim [23], who demonstrated that stronger reactions suppress mass transfer in reactive MHD flows.

Table (1) values are calculated using MATLAB software. The following comparisons are made:

- Skin-friction, Nusselt, and Sherwood coefficients are compared with the Schmidt number.

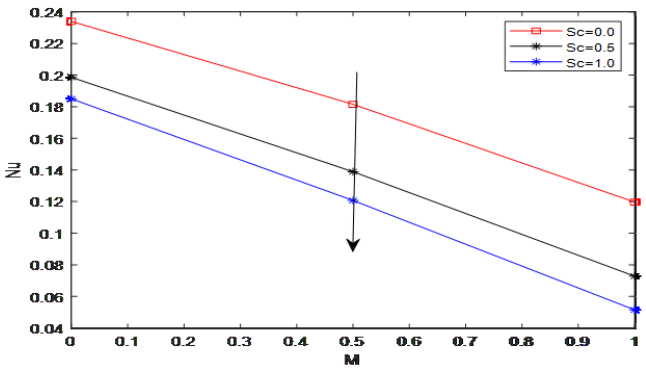

Figure 11: Nusselt number on Schmidt number

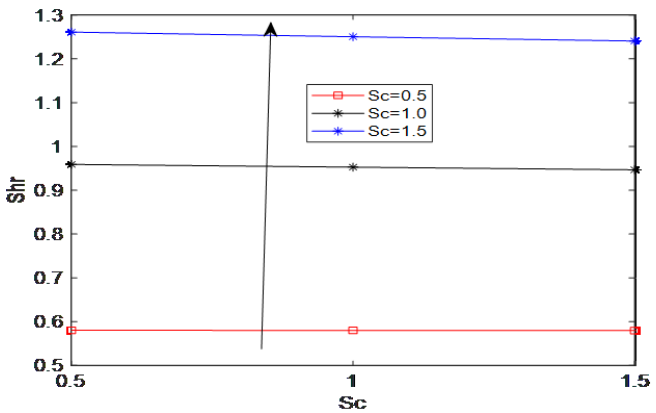

Figure 12: Sherwood values different values of Schmidt number

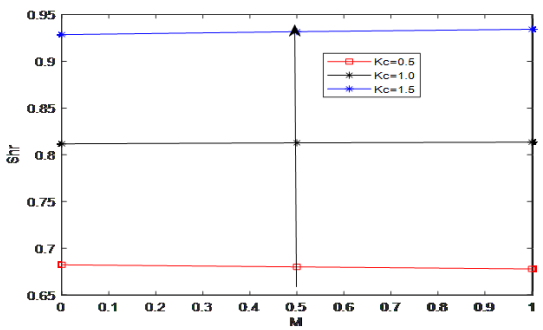

Figure 13: Sherwood number on Chemical Reaction

Table 1: Values of Skin Friction, Nusselt, and Sherwood Numbers

S.No	**Pr**	**Ec**	**N**	**Q**	**Gr**	**Gc**	**Sr**	$\mathbf{K}_c$	**M**	**Sc**	$\mathbf{f''(0)}$	$\theta'(\mathbf{0})$	$\phi'(\mathbf{0})$
1	0.72	0.62	1	0.3	1	1	1	0.5	0.0	0.5	0.14356	0.23402	0.58174
2	0.72	0.62	1	0.3	1	1	1	0.5	0.5	0.5	-0.13278	0.18156	0.58119
3	0.72	0.62	1	0.3	1	1	1	0.5	1.0	0.5	-0.37510	0.11969	0.58040
4	0.72	0.62	1	0.3	1	1	1	0.5	0.0	1.0	0.06000	0.19863	0.95831
5	0.72	0.62	1	0.3	1	1	1	0.5	0.5	1.0	-0.20524	0.13890	0.95202
6	0.72	0.62	1	0.3	1	1	1	0.5	1.0	1.0	-0.43837	0.07279	0.94611
7	0.72	0.62	1	0.3	1	1	1	0.5	0.0	1.5	0.01193	0.18503	1.25985
8	0.72	0.62	1	0.3	1	1	1	0.5	1.0	1.5	-0.24857	0.12069	1.24962
9	0.72	0.62	1	0.3	1	1	1	0.5	1.5	1.5	-0.47748	0.05145	1.24027
10	0.72	0.62	1	0.3	1	1	1	0.5	0.0	0.62	0.11791	0.23402	0.68221
11	0.72	0.62	1	0.3	1	1	1	0.5	0.5	0.62	-0.15463	0.18156	0.68004
12	0.72	0.62	1	0.3	1	1	1	0.5	1.0	0.62	-0.39390	0.11969	0.67780
13	0.72	0.62	1	0.3	1	1	1	1.0	0.0	0.62	0.09272	0.22304	0.81174
14	0.72	0.62	1	0.3	1	1	1	1.0	0.5	0.62	-0.17806	0.16748	0.81281
15	0.72	0.62	1	0.3	1	1	1	1.0	1.0	0.62	-0.41562	0.10334	0.81353
16	0.72	0.62	1	0.3	1	1	1	1.5	0.0	0.62	0.07251	0.21489	0.92863
17	0.72	0.62	1	0.3	1	1	1	1.5	1.0	0.62	-0.19676	0.15705	0.93178
18	0.72	0.62	1	0.3	1	1	1	1.5	1.5	0.62	-0.43290	0.09131	0.93436

- Nusselt and Sherwood coefficients are examined with varying chemical reaction parameters.

5. Conclusions

The results and observations for the above conditions are summarized as follows:

- Fluid velocity and species concentration increase, while temperature decreases, with an increase in the Soret number.
- Fluid velocity decreases with increasing Prandtl number and Soret effect, but increases with a higher heat source parameter.
- Fluid temperature rises with increasing heat source and viscous dissipation, but decreases with higher Prandtl number, Grashof numbers, Soret effect, and chemical reaction parameter.
- Concentration increases with the Soret number, but decreases with higher heat source parameter, Grashof numbers, and chemical reaction parameter.
- The Nusselt number increases, whereas the Sherwood number decreases with a higher Schmidt number, and the skin-friction coefficient decreases with increasing chemical reaction parameter.

6. Further Research / Application

- Future research may focus on multiphase flow, incorporating density and pressure gradient effects.
- Advanced fluid models such as nanofluids, non-Newtonian fluids, and viscoelastic fluids may be investigated.
- Modern computational techniques such as machine learning and artificial intelligence can be incorporated for enhanced analysis.

Nomenclature

Table 2: *

u	Velocity of the plate [m s^{-1}]
v	Suction velocity [m s^{-1}]
G	Gravitational force [m s^{-2}]
σ	Electrical conductivity [S m^{-1}]
β_T	Coefficient of thermal expansion [K^{-1}]
β_C	Mass transfer coefficient [(kg m^{-3})$^{-1}$]
θ	Dimensionless temperature
ϕ	Dimensionless concentration
α	Thermal diffusivity [m^2 s^{-1}]
μ	Dynamic viscosity [Pa s]
B_0	Magnetic field strength [T]
Q_0	Heat source parameter [W m^{-3}]
C_s	Concentration susceptibility [m^3 kg^{-1}]
K_c	Chemical reaction parameter [s^{-1}]
D_m	Mass diffusivity [m^2 s^{-1}]
c_p	Specific heat [J kg^{-1} K^{-1}]
U_0, V_0	Constants
Sr	Soret number
M	Magnetic parameter
Pr	Prandtl number
Sc	Schmidt number
Gr	Grashof number
Gc	Modified Grashof number
Ec	Eckert number
C	Concentration of species
C_w	Concentration of fluid at the plate
Nu	Nusselt number
Sh_r	Sherwood number
S_f	Skin friction

References

1. S, Renuka, Malga, Bala S., K, G., and CH, K. K., 2022, "viscous dispassion and chemical reaction impact on axisymmetric flow through a radially extending surface," *Int. J. Math. Trends Technol.*, 68(10), pp. 44–55, https://doi.org/10.14445/22315373/ijmtt-v68i10p507.

2. Srinivasacharya, D., and Jagadeeshwar, P., 2019, "Effect of joule heating on the flow over an exponentially stretching sheet with convective thermal condition," *Math. Sci.*, 13(3), pp. 201–211, https://doi.org/10.1007/s40096-019-0290-8.

3. Ibrahim, S. M., and Suneetha, K., 2016, "Heat source and chemical effects on mhd convection flow embedded in a porous medium with soret, viscous and joules dissipation," *Ain Shams Eng. J.*, 7(2), pp. 811–818, https://doi.org/10.1016/j.asej.2015.12.008.

4. Hayat, T., Qayyum, S., Khan, M. I., and Alsaedi, A., 2018, "Entropy generation in magnetohydrodynamic radiative flow due to rotating disk in presence of viscous dissipation and joule heating," *Phys. Fluids*, 30(1), https://doi.org/10.1063/1.5009611.

5. Mangamma, C., Appidi, L., Malga, B. S., Kumar, P. P., and Matta, S., 2024, "Effect of radiation and viscous dissipation using the galerkin method over a vertical porous plate with variation in temperature," *Heat Transf.*, 53(4), pp. 1709–1725, https://doi.org/10.1002/htj.23012.

6. Mangamma, C., Kumar, P. P., Malga, B. S., and Appidi, L., 2024, "Effect of dufour and chemical reaction on an unsteady magneto-hydrodynamics flow past an exponentially moving plate," *Heat Transf.*, 53, pp. 1689–1708, https://doi.org/10.1002/htj.23010.

7. Sharma, B. K., and Gandhi, R., 2022, "Combined effects of joule heating and non-uniform heat source/sink on unsteady mhd mixed convective flow over a vertical stretching surface embedded in a darcy-forchheimer porous medium," *Propuls. Power Res.*, 11(2), pp. 276–292, https://doi.org/10.1016/j.jppr.2022.06.001.

8. "Awais, M., Bibi, M., Ali, A., Malik, M. Y., Nisar, K. S., and Jamshed, W., 2022, Numerical analysis of mhd axisymmetric rotating bodewadt rheology under viscous dissipation and ohmic heating effects," *Sci. Rep.*, 12(1), https://doi.org/10.1038/s41598-022-13676-2.

9. Nayak, B., Malga, S. R., Goud, G. R., and Kumar, K., 2019, "Chemical reaction effect of an axisymmetric flow over radially stretched sheet," *Propuls. Power Res.*, 8, p. 79, https://doi.org/10.1016/j.jppr.2019.01.002.

10. Suneetha, M., Malga, B. S., Goud, G. R., Appidi, L., and Kumar, P. P., 2023, "Effects of viscous dissipation on mhd free convection flow past a semi-infinite moving vertical porous plate with heat sink and chemical reaction," *Mater. Today Proc.*, pp. 1629–1636, https://doi.org/10.1016/j.matpr.2023.06.108.

11. Ahmed, R., Ali, N., Khan, S. U., and Tlili, I., 2020, "Numerical Simulations for Mixed Convective Hydromagnetic Peristaltic Flow in a Curved Channel with Joule Heating Features," *AIP Adv.*, 10(7). https://doi.org/10.1063/5.0010964.

12. Oni, M. O., and J., B. K., 2021, "Joule Heating and Viscous Dissipation Effect on Electroosmotic Mixed Convection Flow in a Vertical Microchannel Subjected to Asymmetric Heat Fluxes," *Propuls. Power Res.*, 10(1), pp. 83–94. https://doi.org/10.1016/j.jppr.2021.01.001.

13. Goud, B. S., Kumar, P. P., Malga, B. S., and Reddy, Y. D., 2025, "FEM to Study the Radiation, Soret, Dufour Numbers Effect on Heat and Mass Transfer of Magneto-Casson Fluid over a Vertical Permeable Plate in the Presence of Viscous Dissipation," *Waves Random Complex Media*, 35(4), pp. 7928–7949. https://doi.org/10.1080/17455030.2022.2091809.

14. Kumar, P. P., Malga, B. S., Appidi, L., and Mangamma, C., 2024, "Analysis of the Influence of the Soret Number on Axisymmetric Flow through the Application of the Successive Linearization Technique," *Heat Transf.*, pp. 1–10. https://doi.org/10.1002/htj.23249.

15. Sadia, H. M. M., and M. T., 2024, "Modelling Slip Flow of Bingham Fluid Induced by a Porous Revolving Disk with Viscous Dissipation and Joule Heating Effects," *J. Therm. Anal. Calorim.*, 149, pp. 5555–5567. https://doi.org/10.1007/s10973-024-13260-y.

16. Swain, B. K., Parida, B. C., Kar, S., and Senapati, N., 2020, "Viscous Dissipation and Joule Heating Effect on MHD Flow and Heat Transfer Past a Stretching Sheet Embedded in a Porous Medium," *Heliyon*, 6(10), p. e05338. https://doi.org/10.1016/j.heliyon.2020.e05338.

17. Ravuri Mohana Ramana, G. D., et al., 2024, "Numerical Performance of Hall Current and Darcy-Forchheimer Influences on Dissipative Newtonian Fluid Flow over a Thinner Surface," *Case Stud. Therm. Eng.*, 60, p. 104687. https://doi.org/10.1016/j.csite.2024.104687.

18. Turkyilmazoglu, M., 2021, "Nonlinear Problems via a Convergence Accelerated Decomposition Method of Adomian," *Comput. Model. Eng. Sci.*, 127(1), pp. 1–22. https://doi.org/10.32604/cmes.2021.012595.

19. Krishna, M. V., 2024, "Hall and Ion Slip Effects and Chemical Reaction on MHD Rotating Convective Flow Past an Infinite Vertical Porous Plate with Ramped Wall and Uniform Wall Temperatures," *Biomass Conv. Bioref.*, 14, pp. 11647–11664. https://doi.org/10.1007/s13399-022-03160-2.

20. Hussain, M., et al., 2022, "Suction/Blowing Impact on Magneto-Hydrodynamic Mixed Convection Flow of Williamson Fluid through Stretching Porous Wedge with Viscous Dissipation and Internal Heat Generation/Absorption," *Results Eng.*, 16, p. 100709. https://doi.org/10.1016/j.rineng.2022.100709.

21. Shishehbor, B., and Shishehbor, B., 2024, "Analytical Solution of the Steady Magnetohydrodynamic (MHD) Free Convection Flow over a Semi-Infinite Flat Vertical Plate Moving in a Porous Medium with Viscous Dissipation," *Int. J. Smart Energy Technol. Environ. Eng.*, 3(1), pp. 67–89. https://doi.org/10.61186/setee.3.1.67.

22. Mangamma, C., Malga, B. S., Kumar, P. P., Appidi, L., Suresh, P., and Ravi, P. S., 2024, "Magnetohydrodynamic Boundary Layer Flows over a Moving Porous Vertical Plate with Viscous Dissipation and Dufour Effects in the Presence of Heat Source and Chemical Reaction," *J. Adv. Res. Numer. Heat Transf.*, 26(1), pp. 99–113. https://doi.org/10.37934/arnht.26.1.99113.

23. Karim, M. E., Samad, M. A., and Hasan, M. M., 2012, "Dufour and Soret Effect on Steady MHD Flow in Presence of Heat Generation and Magnetic Field Past an Inclined Stretching Sheet," *Open J. Fluid Dyn.*, 2(3), pp. 91–100. https://doi.org/10.4236/ojfd.2012.23009.

24. Ben Khedher, N., et al., 2024, "Effect of Joule Heating and MHD on Periodical Analysis of Current Density and Amplitude of Heat Transfer of Electrically Conducting Fluid along Thermally Magnetized Cylinder," *Ain Shams Eng. J.*, 15, 102374. https://doi.org/10.1016/j.asej.2023.102374.

[1] *Cheruvu Rajeswari Sowmya, Department of Mathematics, GITAM University, Hyderabad, India.*

email: sowmya.cheruvu@gmail.com

[2] *Bala Siddulu Malga, Department of Mathematics, GITAM University, Hyderabad, India.*

email: drbsmalga@gmail.com

[3] *Gudipalli Deepa, Department of Mathematics, Chaitanya Bharathi Institute of Technology, Hyderabad, India.*

email: gdeepa_maths@cbit.ac.in

[4] *Gitti Narsimlu, Department of Mathematics, Chaitanya Bharathi Institute of Technology, Hyderabad, India.*

email: gnarsimlu_maths@cbit.ac.in